

Near-inflection point inflation and production of dark matter during reheating

Anish Ghoshal

Institute of Theoretical Physics, Faculty of Physics, University of Warsaw,
ul. Pasteura 5, 02-093 Warsaw, Poland,
email: anish.ghoshal@fuw.edu.pl

Gaetano Lambiase

Dipartimento di Fisica "E.R. Caianiello", Universita' di Salerno, I-84084 Fisciano (Sa), Italy
Gruppo Collegato di Salerno, I-84084 Fisciano (Sa), Italy
email:lambiase@sa.infn.it

Supratik Pal

Physics and Applied Mathematics Unit, Indian Statistical Institute, Kolkata-700108, India
Technology Innovation Hub on Data Science, Big Data Analytics and Data Curation, Indian
Statistical Institute, Kolkata-700108, India
email:supratik@isical.ac.in

Arnab Paul

Physics and Applied Mathematics Unit, Indian Statistical Institute, Kolkata-700108, Indi
School of Physical Sciences, Indian Association for the Cultivation of Science, Kolkata-700032,
India

email:arnabpaul9292@gmail.com

Shiladitya Porey*

Department of Physics and Astronomy, Novosibirsk State University,
email: shiladitya@mailbox@gmail.com

Abstract

We study slow roll single field inflationary scenario and the production of non-thermal fermionic dark matter, together with standard model Higgs, during reheating. For the inflationary scenario, we have considered two models of polynomial potential – one is symmetric about the origin and another one is not. We fix the coefficients of the potential from the current Cosmic Microwave Background (CMB) data from Planck/BICEP. Next, we explore the allowed parameter space on the coupling (y_χ) with inflaton and mass (m_χ) of dark matter (DM) particles (χ) produced during reheating and satisfying CMB and several other cosmological constraints.

1 Introduction

Cosmic inflation which is postulated as a fleeting cosmological epoch, occurred at the very early time of the universe. During this primordial epoch, spacetime expanded exponentially resulting in statistical homogeneity and isotropy on large angular scales, the exceedingly flat universe, and providing a proper explanation for the horizon problem. In addition to that, inflation can generate quantum fluctuations, which transform into scalar and tensor perturbations. Scalar perturbation acts as the mechanism for the formation of the large-scale structure, while tensor perturbation is responsible for generating gravitational wave. The

*corresponding author

simplest way to fabricate such an epoch is to assume that the universe was dominated by the energy density of a single scalar field, called inflaton, minimally coupled to gravity and having canonical kinetic energy, slowly rolling along the slope of the potential. However, current data from CMB measurements, e.g. *Planck* [1] and BICEP [2], favour plateau-like potential over the inflaton-potential of the form $V(\phi) \propto \phi^p$ with $p \geq 1$. One of the other alternatives to get such a potential is to consider inflection-point inflation.

On the other hand, CMB measurements suggest that approximately one-quarter of the total mass-energy density of the present universe is in the form of Dark Matter (DM) whose true nature is still not known with certainty. All proposed possible particles of DM can be categorized into two groups - Weakly Interacting Massive Particles (WIMP) and Feebly Interacting Massive Particles (FIMP). Till now, the signature of the presence of WIMP particles has not been detected in particle detector experiments [3]. In that case, FIMP which were never in thermal equilibrium with the relativistic plasma of the universe, seems more favorable as the viable DM candidate [4].

In the paper [5] we studied a single unified model of inflation and the production of non-thermal dark matter particles. For the inflationary part, we have considered two small-field inflection point inflationary scenarios. We have also assumed direct coupling between the inflaton and the DM, a vector-like fermionic field χ which transforms as gauge singlet under the SM gauge groups. The inflaton either decays to DM or may undergo scattering with the dark sector to produce the observed relic. As we will see, additional irreducible gravitational interaction may also mediate the DM production, either by 2-to-2 annihilation of the Standard Model (SM) Higgs bosons or of the inflatons during the reheating era.

This paper is organized as follows: in Section 2, we discuss the condition of getting an inflection point for a single field potential. In Section 3, we study the slow roll inflationary scenario for two potentials and find the location of inflection point and fix the coefficients of the potentials from CMB data. Reheating and production of dark matter have been discussed in Section 5. Section 6 contains conclusion.

2 Inflection-point inflation models

Near the location of the inflection point, the potential takes a plateau-like shape. Because of that, inflection point of the inflationary potential is important for the slow roll inflationary scenario. If inflaton starts rolling along the potential from the vicinity of the inflection point, the number of e-foldings (described in Section 3) increases without significant change in the inflaton value.

To determine the stationary inflection point of an inflationary potential $\mathcal{V}(\psi)$ of a single scalar field ψ , we need the solution of

$$\frac{d\mathcal{V}}{d\psi} = \frac{d^2\mathcal{V}}{d\psi^2} = 0. \quad (1)$$

In the following sections (Section 3) we discuss two different slow roll small-field inflationary scenarios, where each of the inflationary potentials possesses an inflection point.

3 Slow roll inflationary scenario

The Lagrangian density we are interested in, is given by in $\hbar = c = k_B = 1$ unit,

$$\mathcal{L}_I = \frac{M_P^2}{2}\mathcal{R} + \mathcal{L}_{KE,INF} + U_{INF} + \mathcal{L}_{KE,\chi} - U_\chi(\chi) + \mathcal{L}_{KE,H} - U_H(H) + \mathcal{L}_{reh}, \quad (2)$$

where $M_P \simeq 2.4 \times 10^{18}$ GeV is the reduced Planck mass and \mathcal{R} is the Ricci scalar with metric-signature $(+, -, -, -)$. $\mathcal{L}_{KE,INF}$ and U_{INF} are respectively the kinetic energy and potential energy term of the single scalar inflaton. Since, those two terms are function of inflaton, they alter when we change the model of inflation. In this work, we use Φ to symbolize inflaton for Model I inflation and φ for Model II. Accordingly,

$$U_{INF} \equiv \begin{cases} U_\Phi = V_0 + a\Phi - b\Phi^2 + d\Phi^4 & \text{(for Model I),} \\ U_\varphi = p\varphi^2 - q\varphi^4 + w\varphi^6 & \text{(for Model II).} \end{cases} \quad (3a)$$

$$(3b)$$

Here V_0 , a , b , d , p , q , and w are all assumed to be positive, real; and we choose $d, w > 0$. The potential of Eq. (3a) contains a term of linear order of inflaton. Due to this term U_Φ is not symmetric about the origin. On the contrary, the U_φ is symmetric about the origin. In Eq. (2), $\mathcal{L}_{KE,\chi}$, and $\mathcal{L}_{KE,H}$ represent the kinetic energy of the vector-like fermionic DM, χ , and Standard Model (SM) Higgs field, H , respectively. And the potential term for χ and H are given by -

$$U_\chi(\chi) = m_\chi \bar{\chi}\chi, \quad (4)$$

$$U_H(H) = -m_H^2 H^\dagger H + \lambda_H (H^\dagger H)^2. \quad (5)$$

Furthermore, the last term on the right side of Eq. (2), \mathcal{L}_{reh} , takes care of the interactions of χ and H with $\Phi(\varphi)$ during reheating and it is defined as

$$\mathcal{L}_{reh} \equiv \begin{cases} \mathcal{L}_{reh,I} = -y_\chi \Phi \bar{\chi}\chi - \lambda_{12} \Phi H^\dagger H - \lambda_{22} \Phi^2 H^\dagger H & \text{(for Model I),} \\ \mathcal{L}_{reh,II} = -y_\chi \varphi \bar{\chi}\chi - \lambda_{12} \varphi H^\dagger H - \lambda_{22} \varphi^2 H^\dagger H & \text{(for Model II),} \end{cases} \quad (6a)$$

$$(6b)$$

where λ_{12} , λ_{22} , and Yukawa-like y_χ are the couplings of SM Higgs and fermionic DM with inflaton.

During the slow roll inflationary epoch, contribution from the terms except the first three terms in Eq. (2) is negligible. The slow-roll condition is measured in terms of four potential-slow-roll parameters - ϵ_V , η_V , ξ_V , and σ_V . During slow roll inflationary epoch, $|\epsilon_V|, |\eta_V|, |\xi_V|, |\sigma_V| \ll 1$. These four potential-slow-roll parameters for Model I are defined as

$$\epsilon_V \approx \frac{M_P^2}{2} \left(\frac{U'_\Phi}{U_\Phi} \right)^2 = M_P^2 \frac{(a - 2b\Phi + 4d\Phi^3)^2}{2(\Phi(a - b\Phi + d\Phi^3) + V_0)^2}, \quad (7)$$

$$\eta_V \approx M_P^2 \frac{U''_\Phi}{U_\Phi} = -M_P^2 \frac{2(b - 6d\Phi^2)}{\Phi(a - b\Phi + d\Phi^3) + V_0}, \quad (8)$$

$$\xi_V \approx M_P^4 \frac{U'_\Phi U''_\Phi}{U_\Phi^2} = M_P^4 \frac{24d\Phi(a - 2b\Phi + 4d\Phi^3)}{(\Phi(a - b\Phi + d\Phi^3) + V_0)^2}, \quad (9)$$

$$\sigma_V \approx M_P^6 \frac{U'^2_\Phi U''''_\Phi}{U_\Phi^3} = M_P^6 \frac{24d(a - 2b\Phi + 4d\Phi^3)^2}{(\Phi(a - b\Phi + d\Phi^3) + V_0)^3}. \quad (10)$$

Here, prime denotes derivative with respect to inflaton. For Model II inflation, the potential-slow-roll parameters are

$$\epsilon_V = M_P^2 \frac{2(p\varphi - 2q\varphi^3 + 3w\varphi^5)^2}{(p\varphi^2 - q\varphi^4 + w\varphi^6)^2}, \quad (11)$$

$$\eta_V = M_P^2 \frac{2(p - 6q\varphi^2 + 15w\varphi^4)}{p\varphi^2 - q\varphi^4 + w\varphi^6}, \quad (12)$$

$$\xi_V = M_P^4 \frac{48\varphi^2(-q + 5w\varphi^2)(p - 2q\varphi^2 + 3w\varphi^4)}{(p\varphi^2 - q\varphi^4 + w\varphi^6)^2}, \quad (13)$$

$$\sigma_V = M_P^6 \frac{96(-q + 15w\varphi^2)(p\varphi - 2q\varphi^3 + 3w\varphi^5)^2}{(p\varphi^2 - q\varphi^4 + w\varphi^6)^3}. \quad (14)$$

By the time any one of these slow-roll parameters becomes ~ 1 at $\Phi \sim \Phi_{\text{end}}$ (for Model I) or at $\varphi \sim \varphi_{\text{end}}$ (for Model II), slow roll inflation terminates. The duration of slow roll inflation is measured in terms of the total number of e-foldings, $\mathcal{N}_{\text{CMB,tot}}$ as

$$\mathcal{N}_{\text{CMB,tot}} = M_P^{-2} \int_{\Phi_{\text{end}}(\varphi_{\text{end}})}^{\Phi_{\text{CMB}}(\varphi_{\text{CMB}})} \frac{U_{\text{INF}}}{U'_{\text{INF}}} d\Phi(\varphi) = \int_{\Phi_{\text{end}}(\varphi_{\text{end}})}^{\Phi_{\text{CMB}}(\varphi_{\text{CMB}})} \frac{1}{\sqrt{2\epsilon_V}} d\Phi(\varphi), \quad (15)$$

where $\Phi_{\text{CMB}}(\varphi_{\text{CMB}})$ is the inflaton value at which the length scale, which had previously left the causal horizon during inflation, has reentered during the period of recombination.

Moreover, inflation generates primordial scalar and tensor perturbations. The primordial scalar and tensor power spectrum for ' k '-th Fourier mode are defined as

$$\mathcal{P}_s(k) = A_s \left(\frac{k}{k_*} \right)^{n_s - 1 + (1/2)\alpha_s \ln(k/k_*) + (1/6)\beta_s (\ln(k/k_*))^2}, \quad (16)$$

$$\mathcal{P}_h(k) = A_t \left(\frac{k}{k_*} \right)^{n_t + (1/2)dn_t/d\ln k \ln(k/k_*) + \dots}, \quad (17)$$

where $k_* = 0.05 \text{Mpc}^{-1}$; n_s and n_t are the scalar and tensor spectral index, α_s is the running of scalar spectral index, and β_s is called the 'running of running'. Moreover, in Eq. (16)-(17), A_s and A_t are the normalizations. The relation between A_s and inflationary potential is

$$A_s \approx \frac{U_{\text{INF}}}{24\pi^2 M_P^4 \epsilon_V} \approx \frac{2U_{\text{INF}}}{3\pi^2 M_P^4 r}. \quad (18)$$

Here, r is the tensor-to-scalar ratio. r , n_s , α_s and β_s depend on potential-slow-roll parameters as

$$r = \frac{A_t}{A_s} \approx 16\epsilon_V. \quad n_s = \frac{d \ln \mathcal{P}_s}{d \ln k} = 1 + 2\eta_V - 6\epsilon_V, \quad (19)$$

$$\alpha_s \equiv \frac{dn_s}{d \ln k} = 16\epsilon_V \eta_V - 24\epsilon_V^2 - 2\xi_V. \quad (20)$$

$$\beta_s \equiv \frac{d^2 n_s}{d \ln k^2} = -192\epsilon_V^3 + 192\epsilon_V^2 \eta_V - 32\epsilon_V \eta_V^2 - 24\epsilon_V \xi_V + 2\eta_V \xi_V + 2\sigma_V. \quad (21)$$

The observed values of all these inflation parameters measured at $\Phi = \Phi_{\text{CMB}}$ (at $k_* \simeq 0.05 \text{Mpc}^{-1}$) from *Planck*, *WMAP*, and other CMB observations are presented in Table 1. ¹

¹T and E corresponds to temperature and E-mode polarisation of CMB.

Table 1: *CMB constraints on inflationary parameters.*

$\ln(10^{10}A_s)$	3.047 ± 0.014	68%, TT,TE,EE+lowE+lensing+BAO	[1]
n_s	0.9647 ± 0.0043	68%, TT,TE,EE+lowE+lensing+BAO	[1]
$dn_s/d \ln k$	0.0011 ± 0.0099	68%, TT,TE,EE+lowE+lensing+BAO	[1]
$d^2n_s/d \ln k^2$	0.009 ± 0.012	68%, TT,TE,EE+lowE+lensing+BAO	[1]
r	$0.014^{+0.010}_{-0.011}$ and < 0.036	95%, BK18, BICEP3, <i>Keck Array</i> 2020, and WMAP and <i>Planck</i> CMB polarization	[1, 2, 7, 8]

3.1 Estimating coefficients from CMB data

In this subsection, we find the location of inflection points and also, fix the coefficient of the potentials of both inflationary models, mentioned in Eq. (3a) and Eq. (3b), from the CMB data. At first, we start the calculation with Model I. Solution of Eq. (1) provides the location of inflection point for Model I potential

$$\Phi_0 = \frac{3a}{4b} \quad \text{when } d = \frac{8b^3}{27a^2}. \quad (22)$$

To fix the coefficients of the potential of Eq. (3a), following [9, 10], we can write

$$\begin{pmatrix} \Phi_{\text{CMB}} & \Phi_{\text{CMB}}^2 & \Phi_{\text{CMB}}^4 \\ 1 & 2\Phi_{\text{CMB}} & 4\Phi_{\text{CMB}}^3 \\ 0 & 2 & 12\Phi_{\text{CMB}}^2 \end{pmatrix} \begin{pmatrix} a \\ b \\ d \end{pmatrix} = \begin{pmatrix} U_{\Phi}(\Phi_{\text{CMB}}) - V_0 \\ U'_{\Phi}(\Phi_{\text{CMB}}) \\ U''_{\Phi}(\Phi_{\text{CMB}}) \end{pmatrix}, \quad (23)$$

where d is known from Eq. (22) and $U_{\Phi}(\Phi_{\text{CMB}})$, $U'_{\Phi}(\Phi_{\text{CMB}})$ and $U''_{\Phi}(\Phi_{\text{CMB}})$ can be derived using Eq. (7), (8), (9), (18), (19) as

$$U_{\Phi}(\Phi_{\text{CMB}}) = \frac{3}{2} A_s r \pi^2 M_P^4, \quad (24)$$

$$U'_{\Phi}(\Phi_{\text{CMB}}) = \frac{3}{2} \sqrt{\frac{r}{8}} (A_s r \pi^2) M_P^3, \quad (25)$$

$$U''_{\Phi}(\Phi_{\text{CMB}}) = \frac{3}{4} \left(\frac{3r}{8} + n_s - 1 \right) (A_s r \pi^2) M_P^2. \quad (26)$$

Using these together with Table 1, we can find the coefficients of the potential. However, for cosmological purpose, it is adequate to design the potential in a way such that Φ_{CMB} is adjacent to Φ_0 [11]. In order to implement this, let us modify the potential (Eq. (3a)) as

$$U_{\Phi}(\Phi) = V_0 + A \Phi - B \Phi^2 + d \Phi^4, \quad (27)$$

with $A = a(1 - \beta_1^I)$, $B = b(1 - \beta_2^I)$ (where β_1^I, β_2^I are dimensionless) and in the limit $\beta_1^I, \beta_2^I \rightarrow 0$, the slope of the potential vanishes at Φ_0 . Using this modification, we have found the benchmark value for this potential which is exhibited in Table 2, and using this value, the evolution of the potential and slow roll parameters with Φ are illustrated in Fig. 1. From this Fig. 1 it is clear that $\sigma_V, \xi_V, \epsilon_V < |\eta_V|$. Besides, at $\Phi = \Phi_{\text{CMB}}$, $\epsilon_V, |\eta_V|, \xi_V, \sigma_V \ll 1$, and at $\Phi = \Phi_{\text{end}}$, $|\eta_V| \simeq 1$. This last condition leads to the ending of slow roll phase.

Table 2: Benchmark value for linear term potential (Model I) (Φ_{\min} is the minimum of potential in Eq. (27))

V_0/M_P^4	a/M_P^3	b/M_P^2	d	β_1^I	β_2^I
2.788×10^{-19}	9.29×10^{-19}	6.966×10^{-18}	1.16×10^{-16}	6×10^{-7}	6×10^{-7}
Φ_{CMB}/M_P		Φ_{end}/M_P	Φ_{min}/M_P	Φ_0/M_P	
0.1		0.098889	-0.200045	0.100022	
r	n_s	A_s	e-folding	α_s	β_s
9.87606×10^{-12}	0.960249	2.10521×10^{-9}	53.75	-1.97×10^{-3}	-3.92×10^{-5}

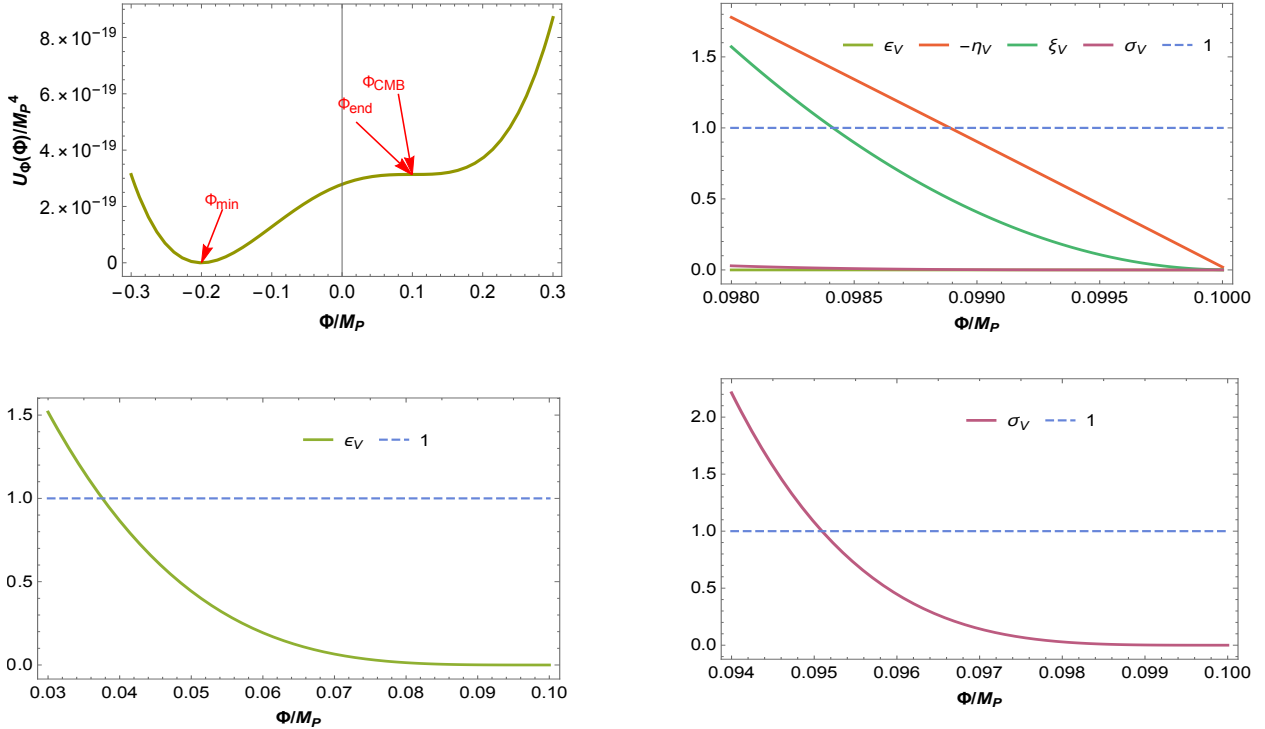


Figure 1: In the top-left panel: normalised inflaton-potential of Model I inflation as a function of ' φ/M_P ' for benchmark value shown in Table 2. The evolution of inflationary slow-roll parameters ($\epsilon_V, -\eta_V, \xi_V, \sigma_V$) as a function of Φ/M_P is presented in the top-right panel; second row - left panel: ϵ_V , and second row - right panel: σ_V of Model I slow roll inflation against Φ/M_P are shown individually for benchmark values listed in Table 2. The dashed line is for 1. Whenever $|\eta_V|$ becomes ~ 1 , the slow roll inflation ends. From these figures, it is clearly visible that $|\epsilon_V| < |\sigma_V| < |\xi_V| < |\eta_V|$ during the slow-roll regime.

Next, we follow similar steps for the inflationary potential of Model II. The potential of Eq. (3b) has an inflection point at

$$\varphi_0 = \frac{\sqrt{q}}{\sqrt{3w}} \quad \text{for } p = \frac{q^2}{3w}. \quad (28)$$

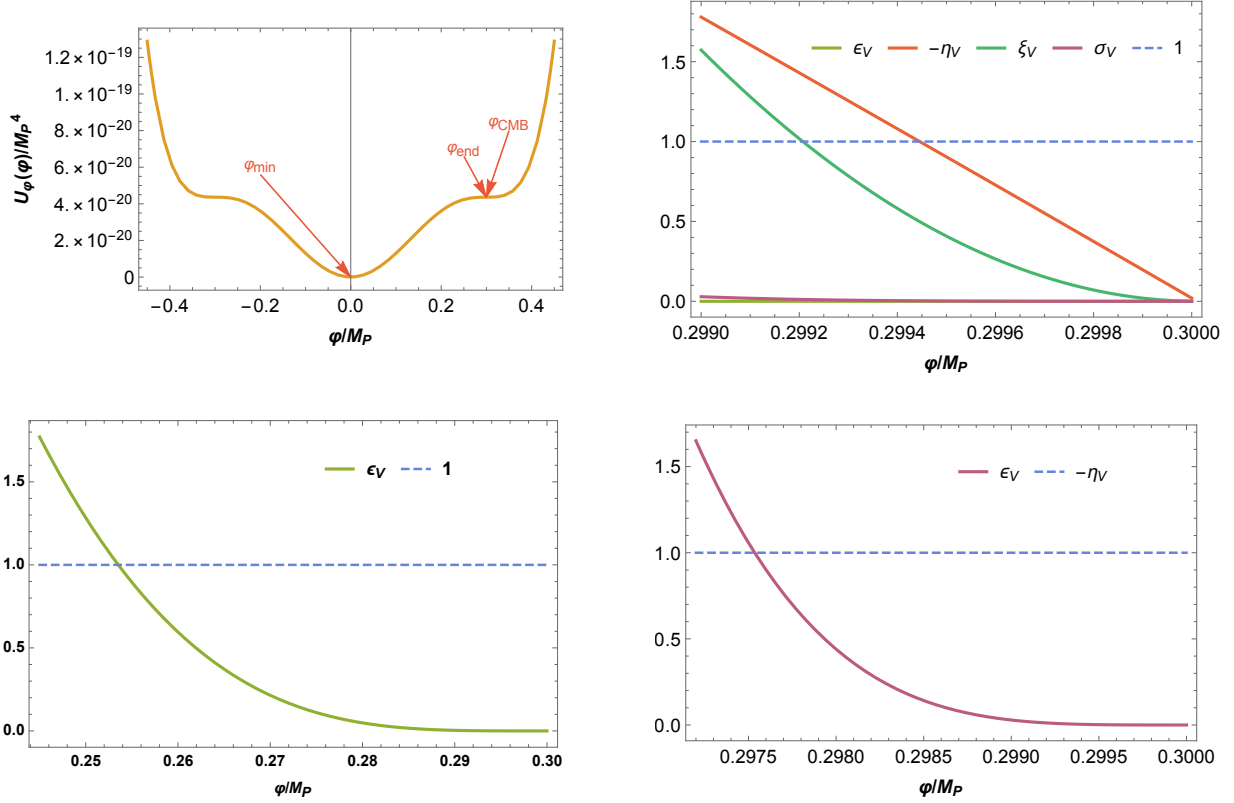


Figure 2: *Top-left panel: evolution of normalised inflaton-potential of Model II for benchmark value from Table 3. Top-right panel: absolute values of four slow roll parameters ($\epsilon_V, -\eta_V, \xi_V, \sigma_V$) are plotted against φ/M_P . Left and right panel of the second row displays ϵ_V and σ_V , respectively, against φ/M_P for benchmark values mentioned in Table 3. The dashed line indicates 1. These graphs demonstrate that $|\epsilon_V| < |\sigma_V| < |\xi_V| < |\eta_V| < 1$ during the slow-roll inflation, similar to what we have found in Model I.*

Likewise, we can also redefine the potential Model II as

$$U_\varphi(\varphi) = p\varphi^2 - Q\varphi^4 + W\varphi^6, \quad (29)$$

such that $Q = q(1 - \beta_1^{II})$ and $W = w(1 - \beta_2^{II})$ and $\beta_1^{II}, \beta_2^{II}$ have zero mass dimension. Then, we can estimate p, q and w , and the values are mentioned in Table 3. For this value, the variation of $U_\varphi(\varphi)$ of Eq. (29) and $\epsilon_V, |\eta_V|, \xi_V, \sigma_V$ as a function of φ is shown in Fig. 2. The slow roll inflationary phase ends at φ_{end} when $|\eta_V| \simeq 1$ (because for Model II $\epsilon_V < |\eta_V|$).

Table 3: *Benchmark values for sextic potential (φ_{min} is the minimum of potential Eq. (29))*

p/M_P^2	q	wM_P^2	β_1^{II}	β_2^{II}	
1.45×10^{-18}	1.62×10^{-17}	5.98×10^{-17}	1.53×10^{-8}	1.53×10^{-8}	
φ_{CMB}/M_P	φ_{end}/M_P	φ_{min}/M_P	φ_0/M_P		
0.3	0.299444	0	0.300011		
r	n_s	A_s	e-folding	α_s	β_s
1.4×10^{-12}	0.96001	2.10521×10^{-9}	60.247	-1.487×10^{-3}	-2.972×10^{-5}

4 Stability analysis

In this section, we attempt to determine the upper bound of y_χ and λ_{12} so that $\mathcal{L}_{\text{reh},I}$ and $\mathcal{L}_{\text{reh},II}$ do not affect the inflationary scenario set forth in Section 3. The Coleman–Weinberg (CW) radiative correction at 1-loop order to the inflaton-potential is given by [6] -

$$V_{\text{CW}} = \sum_j \frac{n_j}{64\pi^2} (-1)^{2s_j} \tilde{m}_j^4 \left[\ln \left(\frac{\tilde{m}_j^2}{\mu^2} \right) - c_j \right]. \quad (30)$$

Here, $j \equiv H, \chi$ and inflaton; $n_{H,\chi} = 4$, n_j for inflaton is 1. Furthermore, $s_H = 0$, $s_\chi = 1/2$, and $s_{\Phi(\varphi)} = 0$. \tilde{m}_j is inflaton dependent mass of the component j and μ is the renormalization scale, which is taken $\sim \Phi_0$ (for Model I) or φ_0 (for Model II). Besides, $c_j = \frac{3}{2}$. Now, the second derivative of the CW term w.r.t. inflaton is

$$V_{\text{CW}}'' = \sum_j \frac{n_j}{32\pi^2} (-1)^{2s_j} \left\{ \left[\left((\tilde{m}_j^2)' \right)^2 + \tilde{m}_j^2 (\tilde{m}_j^2)'' \right] \ln \left(\frac{\tilde{m}_j^2}{\mu^2} \right) - \tilde{m}_j^2 (\tilde{m}_j^2)'' \right\}. \quad (31)$$

In the next two subsections, we investigate the stability relative to the couplings y_χ and λ_{12} for the two inflation-potentials (Eq. (27)) and Eq. (29)) we have considered.

4.1 Stability analysis for linear term inflation

From Eq. (6a), the field-dependent mass of the χ and H are respectively

$$\tilde{m}_\chi^2(\Phi) = (m_\chi + y_\chi \Phi)^2, \quad (32)$$

$$\tilde{m}_H^2(\Phi) = m_H^2 + \lambda_{12} \Phi. \quad (33)$$

For the stability of the inflation-potential, the terms of the order of λ_{12}^2 and y_χ^2 on the right-hand side in Eq. (31) should be less than corresponding tree level terms from Eq. (27)

$$V''_{\text{tree}}(\Phi_0) \equiv U''_{\Phi}(\Phi_0) = \frac{32b^3\Phi_0^2}{9a^2} - 2b(1 - \beta), \quad (34)$$

where $\beta_1^I = \beta_2^I = \beta^I$ (as we have chosen the benchmark value $\beta_1^I = \beta_2^I$). The second derivative (Eq. (31)) of CW term for Higgs field is

$$|V''_{\text{CW},H}| = \frac{\lambda_{12}^2}{8\pi^2} \ln\left(\frac{\lambda_{12}\Phi}{\Phi_0^2}\right). \quad (35)$$

The upper bound of the value of λ_{12} at $\Phi \sim \Phi_0$ can be deduced from $|V''_{\text{CW},H}| < V''_{\text{tree}}(\Phi_0)$, and it is depicted on the right panel of Fig. 3. Thus, allowed value of λ_{12}/M_P is $< 5.283 \times 10^{-12}$.

Similarly, for y_χ ,

$$|V''_{\text{CW},\chi}| = \frac{1}{8\pi^2} \left(6\Phi^2 y_\chi^4 \ln\left(\frac{\Phi^2 y_\chi^2}{\Phi_0^2}\right) - 2\Phi^2 y_\chi^4 \right). \quad (36)$$

The upper bound on y_χ around $\Phi \sim \Phi_0$ can be obtained from $|V''_{\text{CW},\chi}| < V''_{\text{tree}}(\Phi_0)$ which is exhibited on the left panel of Fig. 3, and it gives $y_\chi < 4.578 \times 10^{-6}$.

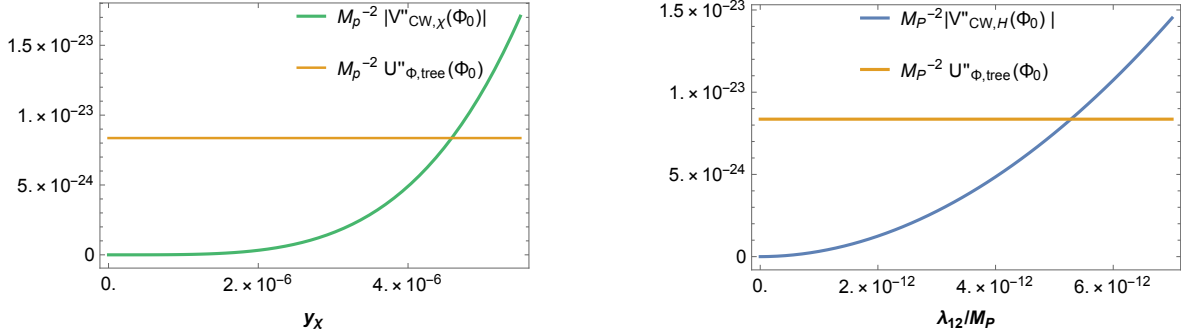


Figure 3: Allowed range for y_χ and λ_{12} for Model I inflation from stability. The yellow colored line represents the value of tree level potential of Model I at Φ_0 . The green and blue colored lines indicate the CW correction due to χ and H , respectively.

4.2 Stability analysis for sextic inflation

In this model, inflaton is φ . Accordingly, the field-depended mass of the fermionic field and Higgs field are respectively

$$\tilde{m}_\chi^2(\varphi) = (m_\chi + y_\chi \varphi)^2, \quad (37)$$

$$\tilde{m}_H^2(\varphi) = m_H^2 + \lambda_{12} \varphi. \quad (38)$$

From Eq. (29)

$$V''_{\text{tree}}(\varphi_0) \equiv U''_{\varphi}(\varphi_0) = \frac{2q^2}{3w} - 12(1 - \beta^{II})q\varphi_0^2 + 30(1 - \beta^{II})w\varphi_0^4, \quad (39)$$

where $\beta_1^{II} = \beta_2^{II} = \beta^{II}$ (because we have chosen $\beta_1^{II} = \beta_2^{II}$ in our benchmark value). Following the steps similar to the ones mentioned in Section 4.1, for λ_{12} Eq. (31) results in

$$|V''_{\text{CW},H}| = \frac{\lambda_{12}^2}{8\pi^2} \ln\left(\frac{\lambda_{12}\varphi}{\varphi_0^2}\right), \quad (40)$$

and for y_χ

$$|V''_{\text{CW},\chi}| = \frac{1}{8\pi^2} \left(6\varphi^2 y_\chi^4 \ln\left(\frac{\varphi^2 y_\chi^2}{\varphi_0^2}\right) - 2\varphi^2 y_\chi^4 \right). \quad (41)$$

In this inflationary case, upper bound on λ_{12} and y_χ around $\varphi \sim \varphi_0$ comes from $|V''_{\text{CW},H}| < V''_{\text{tree}}(\varphi_0)$, and $|V''_{\text{CW},\chi}| < V''_{\text{tree}}(\varphi_0)$, respectively. These have been shown in Fig. 4. The upper bounds are $y_\chi < 6.9 \times 10^{-7}$, and $\lambda_{12}/M_P < 3.58 \times 10^{-13}$.

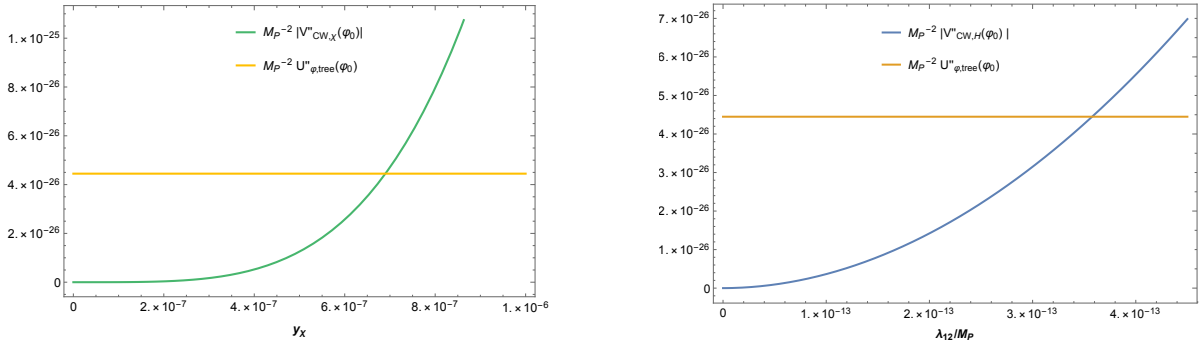


Figure 4: From the stability analysis of Model II inflation, allowed range for y_χ and λ_{12} . The green and blue colored lines result from CW correction for χ and H , and they are compared with the value of tree-level potential of at φ_0 (yellow colored horizontal line).

5 Reheating and Dark Matter

As soon as the slow roll epoch ends, inflaton quickly drops to the minimum of the potential and starts coherent oscillation about that minimum. If Φ_{min} (in Model I) and φ_{min} (in Model II) are the locations of minimum of the inflaton potential respectively, then effective mass of the inflaton in two inflationary models are

$$\frac{m_{\Phi(\varphi)}}{M_P} = \begin{cases} (M_P^{-2} U''_{\Phi}(\Phi)|_{\Phi=\Phi_{\text{min}}})^{1/2} = 6.465 \times 10^{-9} & \text{(for Model I),} \\ (M_P^{-2} U''_{\varphi}(\varphi)|_{\varphi=\varphi_{\text{min}}})^{1/2} = 1.705 \times 10^{-9} & \text{(for Model II).} \end{cases} \quad (42)$$

This oscillating field acts as a non-relativistic fluid without any pressure when averaged over a number of coherent oscillations. The energy density of this inflaton decreases due to two reasons - Hubble expansion and decay to relativistic SM Higgs particle h and DM particle χ following the Lagrangian density of Eq. (6a) and Eq. (6b). The decay width of inflaton to h and χ are

$$\Gamma_{\Phi(\varphi) \rightarrow hh} \simeq \frac{\lambda_{12}^2}{8\pi m_{\Phi(\varphi)}}, \quad \Gamma_{\Phi(\varphi) \rightarrow \chi\chi} \simeq \frac{y_\chi^2 m_{\Phi(\varphi)}}{8\pi}. \quad (43)$$

To satisfy present-day relic density of photons and baryons, we are considering $\Gamma_{\Phi(\varphi)\rightarrow hh} > \Gamma_{\Phi(\varphi)\rightarrow\chi\chi}$ such that total decay width of inflaton $\Gamma = \Gamma_{\Phi(\varphi)\rightarrow\chi\chi} + \Gamma_{\Phi(\varphi)\rightarrow hh} \simeq \Gamma_{\Phi(\varphi)\rightarrow hh}$. Hence,

$$\Gamma = \begin{cases} 6.15 \times 10^6 \frac{\lambda_{12}^2}{M_P^2} & \text{(for Model I),} \\ 2.33 \times 10^7 \frac{\lambda_{12}^2}{M_P^2} & \text{(for Model II).} \end{cases} \quad (44)$$

Now, the branching ratio for the production of χ is

$$\text{Br} = \frac{\Gamma_{\Phi(\varphi)\rightarrow\chi\chi}}{\Gamma_{\Phi(\varphi)\rightarrow\chi\chi} + \Gamma_{\Phi(\varphi)\rightarrow hh}} \simeq \frac{\Gamma_{\Phi(\varphi)\rightarrow\chi\chi}}{\Gamma_{\Phi(\varphi)\rightarrow hh}} = m_{\Phi(\varphi)}^2 \left(\frac{y_\chi}{\lambda_{12}} \right)^2 \quad (45)$$

$$= \begin{cases} 4.18 \times 10^{-17} \left(\frac{y_\chi}{\lambda_{12}} \right)^2 M_P^2 & \text{(for Model I),} \\ 2.91 \times 10^{-18} \left(\frac{y_\chi}{\lambda_{12}} \right)^2 M_P^2 & \text{(for Model II).} \end{cases} \quad (46)$$

These produced particles cause the development of the local-thermal relativistic fluid of the universe and consequently, raise the temperature of the universe. At the beginning of reheating, due to the small value of couplings to inflaton, $\Gamma < \mathcal{H}(\mathbf{a}_{\text{scale}})$, where $\mathcal{H} \equiv \mathcal{H}(\mathbf{a}_{\text{scale}})$ is the Hubble parameter and $\mathbf{a}_{\text{scale}}$ is the cosmological scale factor. Meanwhile, \mathcal{H} continues to decrease. At the moment when \mathcal{H} becomes $\sim \Gamma$, the temperature of the universe is called as reheating temperature, T_{rh} , and it is can be computed as [12]

$$T_{rh} = \sqrt{\frac{2}{\pi}} \left(\frac{10}{g_\star} \right)^{1/4} \sqrt{M_P} \sqrt{\Gamma} = \begin{cases} 1095.07 \lambda_{12} & \text{(for Model I),} \\ 2132.09 \lambda_{12} & \text{(for Model II).} \end{cases} \quad (47)$$

We have assumed $g_\star = 106.75$. At temperature below T_{rh} , the universe behaves as if it is dominated by relativistic particles [13]. Additionally, we have assumed here that the process of particle production from inflaton is instantaneous [14]. In general, reheating is not an instantaneous process. The maximum temperature of the universe during the whole process of reheating may be many orders greater than T_{rh} and it can be estimated as [14]

$$T_{max} = \Gamma^{1/4} \left(\frac{60}{g_\star \pi^2} \right)^{1/4} \left(\frac{3}{8} \right)^{2/5} \mathcal{H}_I^{1/4} M_P^{1/2}, \quad (48)$$

where \mathcal{H}_I is the value of the Hubble parameter at the beginning of reheating when no particle, including the DM, is produced. This can be taken as

$$\mathcal{H}_I \simeq \begin{cases} \sqrt{\frac{U_\Phi(\Phi_0)}{3M_P^2}} = 3.23 \times 10^{-10} M_P & \text{(for Model I),} \\ \sqrt{\frac{U_\varphi(\varphi_0)}{3M_P^2}} = 1.206 \times 10^{-10} M_P & \text{(for Model II).} \end{cases} \quad (49)$$

The Eq. (47) with $T_{rh} \gtrsim 4\text{MeV}$ puts down the lower limit on λ_{12}

$$\frac{\lambda_{12}}{M_P} \gtrsim \begin{cases} 1.52 \times 10^{-24} & \text{(for Model I),} \\ 7.82 \times 10^{-25} & \text{(for Model II).} \end{cases} \quad (50)$$

From Eq. (48), we can write

$$\frac{T_{max}}{T_{rh}} = \left(\frac{3}{8}\right)^{2/5} \left(\frac{\mathcal{H}_I}{\mathcal{H}(T_{rh})}\right)^{1/4}, \quad (51)$$

where

$$\mathcal{H}(T_{rh}) = \frac{\pi}{3M_P} \sqrt{\frac{g_*}{10}} T_{rh}^2. \quad (52)$$

The allowed ranges for T_{max}/T_{rh} for two inflationary models are shown in Fig. 5. The upper limit for the allowed region comes from Eq. (51) and the lower limit from the fact that $T_{rh} \gtrsim 4\text{MeV}$ which is needed for successful Big Bang nucleosynthesis (BBN) [15].

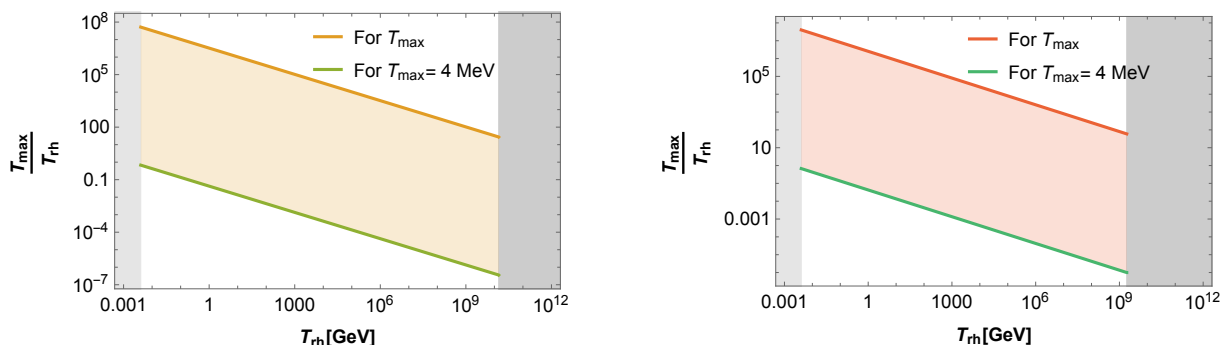


Figure 5: Allowed range (colored region) for T_{max}/T_{rh} : left panel is for Model I inflation, where right panel is for the Model II. The green color line points to T_{max}/T_{rh} when $T_{max} = 4\text{MeV}$. The gray colored area indicates the lower ($T_{rh} \not\geq 4\text{MeV}$) and upper bound on T_{rh} obtained from the stability analysis (see Eq. (35) and Eq. (40)).

5.1 Dark Matter Production and Relic Density

In this subsection, we estimate, following Ref. [12], the amount of DM produced during reheating and compared it with DM relic density of the present-day universe. The Boltzmann equation for the evolution of DM number density, n_χ , of DM particles is -

$$\frac{dn_\chi}{dt} + 3\mathcal{H}n_\chi = \gamma, \quad (53)$$

where t is the physical time, γ is the rate of production of DM per unit volume. Then the evolution equation of comoving number density, $N_\chi = n_\chi \mathbf{a}_{\text{scale}}^3$ ($\mathbf{a}_{\text{scale}}(t)$ is the cosmological scale factor, as mentioned earlier), of DM particles

$$\frac{dN_\chi}{dt} = \mathbf{a}_{\text{scale}}^3 \gamma. \quad (54)$$

While the temperature, T of the universe is $T_{max} > T > T_{rh}$, the energy density of the universe is dominated by inflaton and the first Friedman equation leads to [12]

$$\mathcal{H} = \frac{\pi}{3} \sqrt{\frac{g_*}{10}} \frac{T^4}{M_P T_{rh}^2}. \quad (55)$$

Therefore, energy density of inflaton

$$\rho_{\Phi(\varphi)} = \frac{\pi^2 g_\star}{30} \frac{T^8}{T_{rh}^4}. \quad (56)$$

Since, during reheating, ρ_Φ behaves as a non-relativistic fluids, $\rho_{\Phi(\varphi)} \propto \mathbf{a}_{\text{scale}}^{-3}$, the scale factor behaves as

$$\mathbf{a}_{\text{scale}} \propto T^{-8/3}. \quad (57)$$

Using Eq. (55) and (57) in Eq. (54) we obtain

$$\frac{dN_\chi}{dT} = -\frac{8M_P}{\pi} \left(\frac{10}{g_\star}\right)^{1/2} \frac{T_{rh}^{10}}{T^{13}} \mathbf{a}_{\text{scale}}^3(T_{rh}) \gamma. \quad (58)$$

DM Yield, Y_χ is defined as the ratio of the number density of DM to the entropy density of photons, i.e., $Y_\chi = \frac{n_\chi(T)}{s(T)}$, where entropy density $s(T) = \frac{2\pi^2}{45} g_{\star,s} T^3$ and $g_{\star,s}$ is the effective number of degrees of freedom of the constituents of the relativistic fluid. If we assume that there is no entropy generation in any cosmological process, after reheating epoch, then the evolution of Y_χ can be expressed as

$$\frac{dY_\chi}{dT} = -\frac{135}{2\pi^3 g_{\star,s}} \sqrt{\frac{10}{g_\star}} \frac{M_P}{T^6} \gamma. \quad (59)$$

We are assuming that the DM particles, produced during reheating, were never in thermal equilibrium with the relativistic fluid of the universe. Those DM particles contribute to the cold dark matter (CDM) density of the present universe. Thus, following Table 4, present-day CDM yield [12] is

$$Y_{\text{CDM},0} = \frac{4.3 \times 10^{-10}}{m_\chi}, \quad (60)$$

where m_χ is expressed in GeV. Now, the amount of DM produced during reheating through decay or via scattering in both Model I and Model II, has been estimated and compared with $Y_{\text{CDM},0}$ in the following part of this subsection.

Table 4: *Data about CDM ($h_{\text{CMB}} \approx 0.674$)*

Ω_{CDM}	$0.120 h_{\text{CMB}}^{-2}$	[16]
ρ_c	$1.878 \times 10^{-29} h_{\text{CMB}}^2 \text{gcm}^{-3}$	
s_0	$2891.2 (T/2.7255\text{K})^3 \text{cm}^{-3}$	

5.1.1 Inflaton decay

If DM particles are generated from the inflaton decay

$$\gamma = 2\text{Br} \Gamma \frac{\rho_{\Phi(\varphi)}}{m_{\Phi(\varphi)}}. \quad (61)$$

Substituting this in Eq. (59), the DM yield from the decay of inflaton,

$$Y_{\chi,0} \simeq \frac{3}{\pi} \frac{g_\star}{g_{\star,s}} \sqrt{\frac{10}{g_\star}} \frac{M_P \Gamma}{m_{\Phi(\varphi)} T_{rh}} \text{Br} = \frac{3}{\pi} \frac{g_\star}{g_{\star,s}} \sqrt{\frac{10}{g_\star}} \frac{M_P}{T_{rh}} \frac{(y_\chi)^2}{8\pi} \quad (62)$$

$$= 1.163 \times 10^{-2} M_P \frac{y_\chi^2}{T_{rh}}. \quad (63)$$

Here, we assume $g_{\star,s} = g_\star$. Equating Eq. (63) with Eq. (60), we get the condition to generate the complete CDM energy density -

$$T_{rh} \simeq 6.49 \times 10^{25} y_\chi^2 m_\chi. \quad (64)$$

Fig. 6 depicts the allowed range of the coupling y_χ from Eq. (64), to generate the complete CDM density of the contemporary universe only via the decay channel of inflaton. From this figure, we can deduce that the allowed range for y_χ and m_χ to construct the CDM density of the universe is $10^{-10} \gtrsim y_\chi \gtrsim 10^{-15}$ (for $2.5 \times 10^3 \text{ GeV} \lesssim m_\chi \lesssim 8.1 \times 10^9 \text{ GeV}$ in Model I) and $10^{-11} \gtrsim y_\chi \gtrsim 10^{-15}$ (for $8.4 \times 10^3 \text{ GeV} \lesssim m_\chi \lesssim 2 \times 10^9 \text{ GeV}$ in Model II).

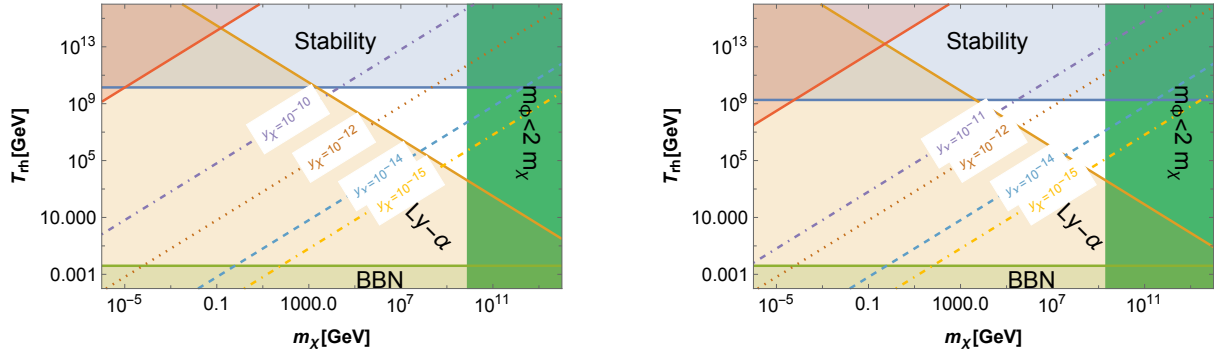


Figure 6: *The allowed region (unshaded) for the Yukawa-like coupling y_χ to produce the complete CDM of the present universe: left panel is for Model I inflation and right for Model II inflation. The constraints (colored regions) are from (a) BBN (light green colored region): $T_{rh} > 4\text{MeV}$, (b) from stability analysis (blue colored region): $T_{rh} \simeq 1.388 \times 10^{10} \text{ GeV}$ (for Model I) or $T_{rh} \simeq 1.83 \times 10^9 \text{ GeV}$ (for Model II) from the upper bound of λ_{12} from Eq. (35) or Eq. (40), (c) stability (red-colored region): from the upper bound of y_χ from Eq. (36) or Eq. (41), (d) (deep green region): m_χ must be $< m_\Phi/2$ (Model I) or $< m_\varphi/2$ (Model II), (e) (light peach-colored region): Ly- α : $T_{rh} \gtrsim (2m_\Phi)/m_\chi$ or $T_{rh} \gtrsim (2m_\varphi)/m_\chi$ [12].*

5.1.2 DM production from scattering channel

In this work, we consider the 2-to-2 scattering processes which contribute significantly in DM production, as mentioned in [12]. When graviton acts as the mediator for the production of DM particles from non-relativistic inflaton via 2-to-2 scattering, then the DM yield [12]

$$Y_{IS,0} \simeq \frac{g_\star^2}{81920 g_{\star,s}} \sqrt{\frac{10}{g_\star}} \left(\frac{T_{rh}}{M_P}\right)^3 \left[\left(\frac{T_{max}}{T_{rh}}\right)^4 - 1 \right] \frac{m_\chi^2}{m_{\Phi(\varphi)}^2} \left(1 - \frac{m_\chi^2}{m_{\Phi(\varphi)}^2}\right)^{3/2}. \quad (65)$$

In Fig. 7, $Y_{IS,0}$ (actually $m_\chi Y_{IS,0}$ with $m_\chi Y_{CDM,0}$) is compared with $Y_{CDM,0}$ for different m_χ as a function of T_{rh} . Hence, it is shown there that the yield of DM produced via scattering (Eq. (65)) is not significant compared to the present CDM density.

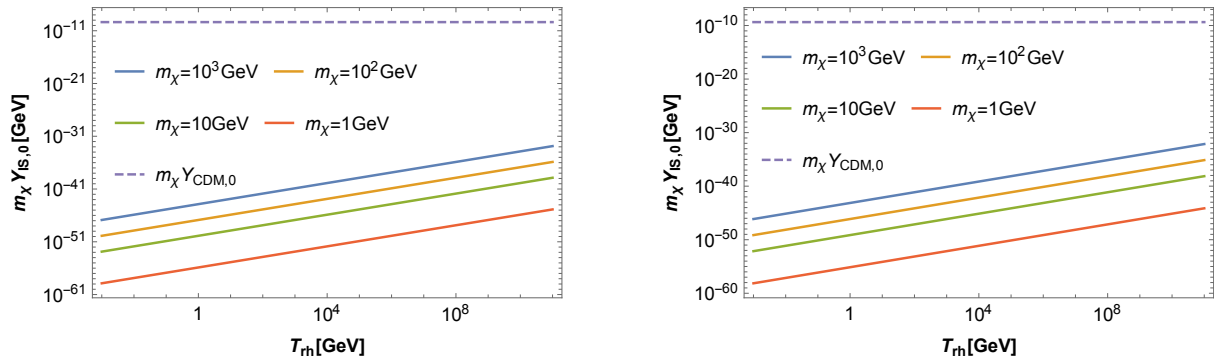


Figure 7: $m_\chi \times$ yield of DM generated from the 2-to-2 scattering with graviton as mediator for different values of m_χ . The left panel shows the result for Model I and the right panel for Model II inflation.

DM particles can also be produced from the scattering of SM particles via graviton mediation. In that case,

$$\gamma = \alpha \frac{T^8}{M_P^4}, \quad (66)$$

where $\alpha \simeq 1.1 \times 10^{-3}$. Due to the presence of M_P^4 in the denominator, it is expected that the production of DM through this process is less compared to previous ones and thus, we neglect.

When inflaton acts as mediator for the production of DM from 2-to-2 scattering of SM particles, production of DM (yield) only through that channel results in

$$Y_{SMi,0} \simeq \frac{135 y_\chi^2 \lambda_{12}^2}{4\pi^8 g_{\star,s}} \sqrt{\frac{10}{g_\star}} \frac{M_P T_{rh}}{m_{\Phi(\varphi)}^4}, \quad \text{for } T_{rh} \ll m_{\Phi(\varphi)}, T_{rh} > T. \quad (67)$$

$Y_{SMi,0} \sim 10^{-60}$ ($\sim 10^{-62}$) for $T_{rh} \sim 10^5 \text{ GeV} \simeq 10^{-5} m_\Phi$ (m_φ) for $g_\star = g_{\star,s} = 106.75$, $\lambda_{12} \sim 10^{-12}$ (10^{-13}) and $y_\chi \sim 10^{-6}$ (10^{-7}). Therefore, the DM produced from 2-to-2 scattering during reheating is insignificant in comparison to total CDM density of the universe.

6 Conclusions and Discussion

We investigated a simple possibility of a scalar inflaton and a non-thermal fermionic particle that originated during the reheating epoch and acted as the CDM. Satisfying the correct relic density of DM and other CMB bounds, we discovered the following features of our analysis:

- We investigated two polynomial potential models for slow roll single field cosmic inflation. Each of these models features an inflection point. Moreover, due to the presence of a term corresponding to the linear power of inflaton (see Eq. (3a)), the potential of Model I is not symmetric about the origin. In contrast, the potential of Model II (Eq. (3b)) is symmetric under the transformation of $\varphi \rightarrow -\varphi$.
- We computed the coefficients of the potentials of both models satisfying the current CMB bounds and under the assumption of near-inflection point inflationary scenario. We also found $n_s \sim 0.96$, $r \sim 10^{-12}$, $\alpha_s \sim 10^{-3}$, and $\beta_s \sim 10^{-8}$ (see Table 2 and Table 3).
- We assumed that inflaton decays to SM Higgs (H) together with DM (χ). From stability analysis of the inflation-potential in Fig. 3 and Fig. 4, we deduced that the upper bounds of the couplings for two decay channels are $\lambda_{12}/M_P \lesssim \mathcal{O}(10^{-12})$ and $y_\chi \lesssim \mathcal{O}(10^{-6})$. The former upper bound defines the highest permissible value of T_{rh} .
- We studied the formation of non-thermal vector-like fermionic DM particles, during reheating from the inflaton decay. The rate of DM creation through this decay is temperature dependent; when the temperature of the universe's relativistic fluid increases during reheating, the rate of DM generation reduces (Eq. (59)). Fig. 5 depicts the permissible range for the ratio of the highest temperature T_{max} to the reheating temperature T_{rh} during that period, T_{max}/T_{rh} . For $T_{rh} = 4\text{MeV}$, the ratio might reach $\mathcal{O}(10^7)$. The permitted range of T_{max}/T_{rh} is determined by the inflection point (see Eq. (48) and Eq. (49)). Because we chose the CMB scale around the inflection point, the inflection point determines the CMB observables, such as n_s and r on one hand, and controls the production regimes (via T_{max}) of DM and consequently DM relic on the other hand.
- Fig. 6 depicts the allowed region in $T_{rh} - m_\chi$ space for two models of potential we have considered and the constraints on that space are coming from bound on T_{rh} from BBN, radiative stability analysis of the potential for slow roll inflation, Ly- α bound, and the maximum possible value of m_χ for the effective mass of the inflaton. From this figure we can conclude that χ produced only through the decay of inflaton may explain the total density of CDM of the current universe if $10^{-10} \gtrsim y_\chi \gtrsim 10^{-15}$ (for $2.5 \times 10^3 \text{ GeV} \lesssim m_\chi \lesssim 8.1 \times 10^9 \text{ GeV}$ in Model I) and $10^{-11} \gtrsim y_\chi \gtrsim 10^{-15}$ (for $8.4 \times 10^3 \text{ GeV} \lesssim m_\chi \lesssim 2 \times 10^9 \text{ GeV}$ in Model II).
- χ can also be produced from 2-to-2 scattering of either SM particles or inflatons. Among all those scattering processes, the promising one is – from the scattering of

inflaton with graviton as the mediator. In Fig. 7 we showed that Y_χ produced through 2-to-2 scattering of inflaton with graviton as mediator, is more than the DM production via other scattering channels, and it is $Y_{IS,0} \sim \mathcal{O}(10^{-36})$ for $T_{rh} = 10^8$ GeV, $m_\chi = 10^3$ GeV. But, $Y_{IS,0}$ produced through this channel is much less than $Y_{\text{CDM},0}$ and thus χ produced through 2-to-2 scattering channels can contribute only a negligible fraction of $Y_{\text{CDM},0}$.

In conclusion, we consider two members of the beyond the standard model physics - inflaton and the non-thermal DM, to connect the CMB data and the DM mystery. This work can be further extended to study the formation of Primordial Black Holes for inflection point inflationary scenario, non-Gaussianities in the CMB spectrum, and generation of Gravitational Waves which can be tested from future CMB experiments.

Acknowledgement

Shiladitya Porey wants to thank Professor Norma Susana Mankoč Borštnik, Professor Maxim Khlopov, Professor Astri Kleppe, and the organizers of the Bled 25th Workshop. Work of Shiladitya Porey is funded by RSF Grant 19-42-02004. Supratik Pal thanks Department of Science and Technology, Govt. of India for partial support through Grant No. NMICPS/006/MD/2020-21.

References

- [1] N. Aghanim *et al.* [Planck], *Astron. Astrophys.* **641**, A6 (2020) [erratum: *Astron. Astrophys.* **652**, C4 (2021)] doi:10.1051/0004-6361/201833910 [arXiv:1807.06209 [astro-ph.CO]].
- [2] P. A. R. Ade *et al.* [BICEP/Keck], [arXiv:2203.16556 [astro-ph.CO]].
- [3] J. Aalbers *et al.* [LZ], [arXiv:2207.03764 [hep-ex]].
- [4] J. Billard, M. Boulay, S. Cebrián, L. Covi, G. Fiorillo, A. Green, J. Kopp, B. Majorovits, K. Palladino and F. Petricca, *et al.* *Rept. Prog. Phys.* **85**, no.5, 056201 (2022) doi:10.1088/1361-6633/ac5754 [arXiv:2104.07634 [hep-ex]].
- [5] A. Ghoshal, G. Lambiase, S. Pal, A. Paul and S. Porey, *JHEP* **09**, 231 (2022) doi:10.1007/JHEP09(2022)231 [arXiv:2206.10648 [hep-ph]].
- [6] M. Drees and Y. Xu, *JCAP* **09**, 012 (2021) doi:10.1088/1475-7516/2021/09/012 [arXiv:2104.03977 [hep-ph]].
- [7] P. A. R. Ade *et al.* [BICEP and Keck], *Phys. Rev. Lett.* **127**, no.15, 151301 (2021) doi:10.1103/PhysRevLett.127.151301 [arXiv:2110.00483 [astro-ph.CO]].
- [8] P. Campeti and E. Komatsu, [arXiv:2205.05617 [astro-ph.CO]].

- [9] S. Hotchkiss, A. Mazumdar and S. Nadathur, JCAP **02**, 008 (2012) doi:10.1088/1475-7516/2012/02/008 [arXiv:1110.5389 [astro-ph.CO]].
- [10] A. Chatterjee and A. Mazumdar, JCAP **01**, 031 (2015) doi:10.1088/1475-7516/2015/01/031 [arXiv:1409.4442 [astro-ph.CO]].
- [11] J. Garcia-Bellido and E. Ruiz Morales, Phys. Dark Univ. **18**, 47-54 (2017) doi:10.1016/j.dark.2017.09.007 [arXiv:1702.03901 [astro-ph.CO]].
- [12] N. Bernal and Y. Xu, Eur. Phys. J. C **81**, no.10, 877 (2021) doi:10.1140/epjc/s10052-021-09694-5 [arXiv:2106.03950 [hep-ph]].
- [13] E. W. Kolb, A. Notari and A. Riotto, Phys. Rev. D **68**, 123505 (2003) doi:10.1103/PhysRevD.68.123505 [arXiv:hep-ph/0307241 [hep-ph]].
- [14] D. J. H. Chung, E. W. Kolb and A. Riotto, Phys. Rev. D **60**, 063504 (1999) doi:10.1103/PhysRevD.60.063504 [arXiv:hep-ph/9809453 [hep-ph]].
- [15] G. F. Giudice, E. W. Kolb and A. Riotto, Phys. Rev. D **64**, 023508 (2001) doi:10.1103/PhysRevD.64.023508 [arXiv:hep-ph/0005123 [hep-ph]].
- [16] P. A. Zyla *et al.* [Particle Data Group], PTEP **2020**, no.8, 083C01 (2020) doi:10.1093/ptep/ptaa104